

X-ray emission from high-redshift miniquasars: self-regulating the population of massive black holes through global warming

Takamitsu Tanaka^{1*}, Rosalba Perna², and Zoltán Haiman³

¹Max-Planck-Institut für Astrophysik, Karl-Schwarzschild-Str. 1, 85741 Garching, Germany

²JILA and Department of Astrophysical and Planetary Science, University of Colorado at Boulder, 440 UCB, Boulder, CO, 80309, USA

³Department of Astronomy, Columbia University, 550 West 120th Street, New York, NY 10027, USA

17 July 2012

ABSTRACT

Observations of high-redshift quasars at $z \gtrsim 6$ imply that supermassive black holes (SMBHs) with masses $M \gtrsim 10^9 M_\odot$ were in place less than 1 Gyr after the Big Bang. If these SMBHs assembled from “seed” BHs left behind by the first stars, then they must have accreted gas at close to the Eddington limit during a large fraction ($\gtrsim 50\%$) of the time. A generic problem with this scenario, however, is that the mass density in $M \sim 10^6 M_\odot$ SMBHs at $z \sim 6$ already exceeds the locally observed SMBH mass density by several orders of magnitude; in order to avoid this overproduction, BH seed formation and growth must become significantly less efficient in less massive protogalaxies through some form of feedback, while proceeding unabated in the most massive galaxies that formed first. Using Monte-Carlo realizations of the merger and growth history of BHs, we show that X-rays from the earliest accreting BHs can provide such a feedback mechanism, on a global scale. Our calculations paint a self-consistent picture of *black-hole-made climate change*, in which the first miniquasars—among them the ancestors of the $z \sim 6$ quasar SMBHs—globally warm the intergalactic medium and suppress the formation and growth of subsequent generations of BHs. We present two specific models with global miniquasar feedback that provide excellent agreement with recent estimates of the $z = 6$ SMBH mass function. For each of these models, we estimate the rate of BH mergers at $z > 6$ that could be detected by the proposed gravitational-wave observatory *eLISA*/NGO.

Key words: black hole physics – cosmology: theory – galaxies: formation – quasars: general – gravitational waves

1 INTRODUCTION

The discovery of bright quasars at redshifts $z \gtrsim 6$ in the Sloan Digital Sky Survey (see the review by Fan 2006), the Canada-France High- z Quasar Survey (Willott et al. 2010a), and the current redshift record-holder at $z = 7.08$ in the UKIDSS (Mortlock et al. 2011) indicates that supermassive black holes (SMBHs) as massive as several $10^9 M_\odot$ were already in place when the Universe was less than 1 Gyr old.

The mechanism by which these early massive BHs formed and grew remains poorly understood (see, e.g., Haiman 2012 for a recent comprehensive review). One class of explanations is the rapid collapse of primordial gas into a $10^4 - 10^6 M_\odot$ black hole, either directly (e.g. Haehnelt & Rees 1993; Loeb & Rasio 1994), by accreting

onto a pre-existing smaller seed BH (e.g. Volonteri & Rees 2005), or by going through the interim state of a very massive star (e.g. Bond, Arnett & Carr 1984), a rapidly accreting massive “proto-star” (Begelman, Volonteri & Rees 2006; Hosokawa, Omukai & Yorke 2012) or a dense stellar cluster (Omukai, Schneider & Haiman 2008; Devecchi & Volonteri 2009). These models rely on rapid gas contraction in deep potential wells (halos with virial temperatures $T_{\text{vir}} \gtrsim 10^4 \text{K}$; Oh & Haiman 2002; Bromm & Loeb 2003; Lodato & Natarajan 2006; Spaans & Silk 2006; Wise & Abel 2008; Regan & Haehnelt 2009; Shang, Bryan & Haiman 2010) and require the gas to avoid fragmenting early on by cooling via H_2 and/or metals. It is unclear whether this special configuration—warm, dense, metal-free gas in relatively massive halos—is realized in nature (Dijkstra et al. 2008; Schleicher, Spaans & Glover

* E-mail: taka@mpa-garching.mpg.de

2010; Petri, Ferrara & Salvaterra 2012; Inayoshi & Omukai 2012; Agarwal et al. 2012).

An alternative possibility, which we explore further in this paper, is that metal-free stars, with masses $\sim 10 - 100 M_{\odot}$, form at redshifts as high as $z \gtrsim 25$ (Abel, Bryan & Norman 2002; Bromm, Coppi & Larson 2002; Yoshida, Omukai & Hernquist 2008), leave behind remnant BHs with similar masses (Heger et al. 2003), and subsequently grow by mergers and by mass accretion near the Eddington limit (Haiman & Loeb 2001; Haehnelt 2003; Bromley, Somerville & Fabian 2004; Yoo & Miralda-Escudé 2004; Taniguchi 2004; Shapiro 2005; Volonteri & Rees 2006; Tanaka & Haiman 2009, hereafter TH09). The primary theoretical uncertainty of this scenario is whether the seed BHs can sustain such high accretion rates.

To reach masses of $> 10^9 M_{\odot}$ by $z \sim 7$, the stellar-mass BHs must grow near the Eddington limit without significant interruption (with a mean duty cycle $\gtrsim 0.5$ at radiative efficiency 0.07; TH09).¹ However, the accretion rates of BHs are limited by their gaseous environments: the rates can be significantly sub-Eddington if the seed mass is light, or if the BH is embedded in a low-density and/or high-temperature medium, as may often be the case at high redshifts (see § 2.1.2). Another limitation is radiative feedback: recent work has shown that the accretion is episodic, with time-averaged Eddington duty cycle of at most $\sim 1/3$ (Milosavljević et al. 2009; Park & Ricotti 2012; see also earlier work by Ciotti & Ostriker 2001 for radiative feedback forcing accretion to be episodic with a low duty cycle at lower redshifts). This local feedback could be mitigated if the flow is non-spherical (i.e., in a disk) and the radiation escapes vertically without compromising the equatorial fuel supply. Finally, a third type of limitation could be the lack of continuous fuel supply on larger scales. Interestingly, Di Matteo et al. (2012) have found that, at least for $\gtrsim 10^5 M_{\odot}$ BHs residing in massive ($\gtrsim 10^9 M_{\odot}$) galaxies at lower redshifts $6 < z < 12$, filamentary accretion of cool gas into the host galaxy may deliver gas to the central regions of massive galaxies near the rates corresponding to the BH's Eddington limit. The large Eddington ratios (~ 1 ; Willott et al. 2010b) and duty cycles ($\gtrsim 0.5$; Shankar et al. 2010) inferred from observations of the quasar SMBHs at $z \sim 6$ appear to be consistent with a sustained and rapid BH growth.

If the BHs can indeed maintain such high accretion rates, then they can grow into $\gtrsim 10^9 M_{\odot}$ SMBHs by $z > 6$. *However, another, less appreciated problem then arises: these optimistic assumptions inevitably lead to a severe over-production for the space density of lower-mass ($10^{5-7} M_{\odot}$) BHs.* The global comoving mass density of SMBHs in galactic nuclei in such models can exceed the locally observed mass density by several orders of magnitude, even if less than 0.1% of star-forming halos form a seed BH (Bromley, Somerville & Fabian 2004; Tanaka & Haiman 2009). The overproduction can be avoided if the growth of lower-mass nuclear BHs is suppressed at late times, e.g. by imposing an early $M - \sigma$ rela-

tion or scaling the BH growth with the host galaxy merger history.

The purpose of the present paper is to consider an alternative solution to this problem. In the SMBH growth models of TH09, the $z \sim 6$ SMBHs originate from seeds born in the first minihalos at redshifts $z \gtrsim 25$. On the other hand, the lower-mass ($M \lesssim 10^7 M_{\odot}$) BHs arise primarily from seeds born inside minihalos collapsing later, at $z \sim 15$. In principle, therefore, the overproduction of the $\gtrsim 10^{5-7} M_{\odot}$ BHs can be avoided, provided that the seed BHs are either unable to form, or unable to grow, in the vast majority of minihalos at $z \lesssim 20$. A natural reason for this could be photoionization heating of the intergalactic medium (IGM) by the earliest accreting seed BHs themselves. The X-rays emitted from these holes have a long mean free path and establish an early X-ray background, which can pre-heat and pre-ionize the IGM (Oh 2001; Venkatesan, Giroux & Shull 2001; Ricotti & Ostriker 2004; Madau et al. 2004). Once this heating sufficiently elevates the IGM gas temperature, the collapse of gas into low-mass halos will be suppressed throughout the Universe.²

We examine whether X-rays produced from the earliest BHs themselves may provide sufficient heating to avoid the overproduction of the $10^{5-7} M_{\odot}$ BHs at $z \sim 6$. Our study extends that of TH09, by self-consistently treating global X-ray heating and the corresponding rise in the halo mass scale for seed formation and BH growth.

This paper is organized as follows. In §2, we describe our modeling the co-evolution of BHs (§2.1) and the thermal and ionization state of the IGM (§2.2). Results of the coupled evolution of BH growth and IGM heating are presented in §3. In §4, we discuss earlier studies on high-redshift miniquasar feedback, and offer general conclusions on viable models of the $z > 6$ quasar SMBHs. Finally, we summarize our main conclusions in §5.

2 METHODS

We couple a merger-tree BH assembly model with radiative-transfer calculations of the global heating and ionization of the IGM. Our semi-analytic method self-consistently models the intertwined evolution of the entire population of accreting nuclear BHs in halos with masses $M \gtrsim 3 \times 10^4 M_{\odot}$ in the redshift range $6 < z < 45$, with a statistical representation equivalent to ≈ 5 comoving Gpc³.

2.1 Black hole growth

Following earlier work (e.g., Volonteri, Haardt & Madau 2003; Bromley, Somerville & Fabian 2004; Yoo & Miralda-Escudé 2004; Volonteri & Rees 2006; TH09), we compute the hierarchical growth of dark matter (DM) halos by means of Monte Carlo merger trees in the

¹ Alternatively, the accretion could occur intermittently in brief episodes of super-Eddington accretion.

² Another possibility is metal-enrichment: once the IGM is polluted, massive PopIII stars may stop forming, and remnant BHs will become much less common. However, this is less attractive, because the metals will be much more localized around pre-existing sources (at least much more than X-ray photons), and cannot produce a global feedback (though clustering can make metal-feedback more effective; Kramer, Haiman & Oh 2006).

extended Press-Schechter formalism (Lacey & Cole 1993; Somerville & Kolatt 1999; Zhang, Fakhouri & Ma 2008), and couple it with a semi-analytical model to follow the growth and dynamics of BHs. We employ a Λ CDM cosmology with the parameter values $h = 0.704$, $\Omega_\Lambda = 0.728$, $\Omega_m = 0.272$, $\Omega_b = 0.045$ and $\sigma_8 = 0.81$ (Jarosik et al. 2011). We start at $z = 6$ and model the assembly history of the full halo mass function above $M_{\text{halo}} > 10^8 M_\odot$ at this redshift, following the method of TH09. The reader is referred to that paper for a detailed description of the Monte-Carlo algorithm; here we summarize the most important features and highlight the improvements over TH09.

The rarest, most massive halos are simulated individually, which determines the cosmological volume represented by our suite of simulations. The population of less massive halos is divided into logarithmic mass bins of width $\Delta \log(M_{\text{halo}}/M_\odot) = 0.5$; within each bin, a sufficiently large number ($\sim 10^{2-3}$) of unique halos are simulated to obtain a statistical sample for low-mass halos. The BHs in these low-mass halos are then counted multiple times (“cloned”) to represent the same large volume as for the most massive halos. Our most massive bin consists of three halos with $M_{\text{halo}} > 10^{12.7} M_\odot$, from which we infer that our suite of merger trees represents a statistical sample equivalent to a comoving volume of $\sim 5 \text{ Gpc}^3$. Our results are based on a total of $\approx 10^4$ merger trees in each model.

The most significant change relative to TH09 is that we have improved our halo mass resolution to correspond to a virial temperature of $T_{\text{vir}} = 400\text{K}$. Above this value, the gas can collapse through efficient cooling by H_2 (Haiman, Thoul & Loeb 1996; Tegmark et al. 1997; Machacek, Bryan & Abel 2001). We follow the merger history of each halo down to this limit. As a result, our merger trees also extend to higher redshift (as large as $z_{\text{max}} \approx 45$), and to lower masses (as low as $3 \times 10^4 M_\odot$).³

At each redshift, the comoving density $\rho_{\text{BH}}(z)$ of BHs residing in (proto-)galactic nuclei changes due to a combination of three effects: accretion onto the holes already present at redshift z , creation of new seeds in small halos, and ejections due to gravitational recoil;

$$\dot{\rho}_{\text{BH,net}}(z) = \dot{\rho}_{\text{acc}}(z) + \dot{\rho}_{\text{creat}}(z) - \dot{\rho}_{\text{ejc}}(z). \quad (1)$$

BH accretion deposits high-energy photons into the IGM, heating it and affecting the conditions for subsequent BH growth. Below, we describe our model implementation of each of these components.

2.1.1 Seed black hole formation

Starting from the highest redshift in each merger tree, we follow all of the branches of the tree towards lower redshifts. We place seed BHs in halos when they first reach a virial temperature of 400K. This corresponds to a mass threshold

$$M_{\text{halo}}^{\text{(seed)}} \gtrsim 9.1 \times 10^4 \left(\frac{\mu}{1.2}\right)^{-3/2} \left(\frac{1+z}{21}\right)^{-3/2} M_\odot, \quad (2)$$

³ The relative streaming velocities ($1 - 10 \text{ km s}^{-1}$) between baryons and dark matter can increase the mass threshold for halo virialization and delay PopIII star formation (Tseliakhovich, Barkana & Hirata 2011; Greif et al. 2011a; Li, Tanaka and Haiman, in preparation.)

where μ is the mean molecular weight.

The initial mass function (IMF) of the first stars remains highly uncertain. Simulations that include the effects of radiative feedback from the accreting protostar had suggested that the maximum mass is $\approx 320 M_\odot$ (Omukai & Palla 2001; Ohkubo et al. 2009), with recent studies yielding values as low as $30 M_\odot$ (Stacy, Greif & Bromm 2012) to $43 M_\odot$ (Hosokawa et al. 2011). Recent simulations have also suggested that hydrodynamical turbulence in star-forming halos may place *typical* masses of PopIII stars significantly lower than previously believed, perhaps $M_* \gtrsim 10 - 50 M_\odot$; that their IMF was less steep than PopI stars, and that they may have formed in small groups or clusters (Turk, Abel & O’Shea 2009; Stacy, Greif & Bromm 2010; Greif et al. 2011b; Turk et al. 2012; Greif et al. 2012). For our purposes, what matters is only that there is a reasonable chance for forming at least one massive PopIII star in a minihalo that can leave behind a seed BH. For concreteness, we chose an IMF with stellar masses in the range $20 M_\odot < M_* < 320 M_\odot$, with a Salpeter (Salpeter 1955) power-law slope $dn/d\log M_* \propto M_*^{-1.35}$. This choice is conservative in that most of the seed BHs have low masses – but we emphasize that it is still possible that most, or even all, PopIII stars had still lower masses and left no seed BHs.

For simplicity, we also assume that at most one massive star forms per halo, because the halo is metal-polluted once it undergoes a star-formation episode. (This assumption is conservative: massive stars outside the pair instability SN range are thought to collapse directly into a BH without ejecting metals; Heger et al. 2003.) Pristine halos that merge with such halos are also considered to be polluted. We do not allow seed BH formation in metal-polluted halos; we consider such halos to be unable to form massive stars whose BH remnants have masses of more than several M_\odot (Heger et al. 2003).

The seed BH masses are modeled using fitting formulae to the simulation results of Zhang, Woosley & Heger (2008), who calculated the remnant masses of metal-free stars undergoing core-collapse explosions while accounting for the mass of the ejecta that falls back onto the remnant. Specifically, we prescribe

$$M_{\text{BH}} = \begin{cases} \frac{3}{4}(M_* - 20 M_\odot) + 2 M_\odot & \text{if } M_* \leq 45 M_\odot \\ \frac{5}{12}(M_* - 20 M_\odot) & \text{if } M_* > 45 M_\odot \end{cases} \quad (3)$$

and assume that stars in the pair-instability mass range $140 M_\odot < M_* < 260 M_\odot$ leave no BH remnant.

For reference, we note that the above differs from the earlier treatment of TH09, in which all of the BH seeds were assumed to have the same mass of $100 M_\odot$. In the present model, the mean PopIII stellar mass is $\langle M_* \rangle \approx 49 M_\odot$, and the mean seed BH mass is $\langle M_{\text{BH}} \rangle \approx 13 M_\odot$.

2.1.2 Black hole accretion

As our fiducial accretion model, we take a simple scenario in which all seed BHs grow continuously (at least in a time-averaged sense) at a fraction f_{Edd} of the Eddington accretion rate,

$$\dot{M} = f_{\text{Edd}} \dot{M}_{\text{Edd}}; \quad (4)$$

$$\dot{M}_{\text{Edd}} = 2.2 \times 10^{-3} \frac{1-\epsilon}{\epsilon} M_{\text{BH}} \text{ Myr}^{-1} \propto M_{\text{BH}}. \quad (5)$$

Here ϵ is the radiative efficiency, which we take to be 0.07 (cf. Merloni & Heinz 2008; Shankar, Weinberg & Miralda-Escudé 2009). With this prescription all BHs grow exponentially with an e-folding timescale of $34 f_{\text{Edd}}^{-1}$ Myr. We also consider a more realistic prescription in which the accretion rate is further limited by the Bondi rate \dot{M}_{Bondi} , i.e.

$$\dot{M} = \min(f_{\text{Edd}} \dot{M}_{\text{Edd}}, \dot{M}_{\text{Bondi}}); \quad (6)$$

$$\dot{M}_{\text{Bondi}} = 4\pi G^2 M_{\text{BH}}^2 \frac{\rho_{\text{gas}}}{c_s^3} \propto M_{\text{BH}}^2. \quad (7)$$

Here ρ_{gas} and c_s are the gas density and sound speed, respectively. In general, in the cold and dense cores of the cuspy gas density profiles of minihalos, in which gas cools efficiently (Abel, Bryan & Norman 2002; Bromm, Coppi & Larson 2002), the Bondi rate exceeds the Eddington rate, and so does not impose a limitation (Turner 1991; TH09). On the other hand, the growing seed BHs can find themselves in a much lower-density medium for several reasons. First, the progenitor star could have blown most of the gas out of the host halo, so that the seed BH is born in a low-density gas (Whalen, Abel & Norman 2004; Alvarez, Wise & Abel 2009). Second, although the photo-heated gas could cool (via Compton scattering on the CMB) and fall back into the halo, it will retain excess entropy and may not be able to form H_2 and cool again, especially if a strong Lyman-Werner background is present (Haiman, Rees & Loeb 1997; Oh & Haiman 2003). In this case, the gas will be in a pressure-supported configuration at much lower density (e.g. Shapiro, Iliev & Raga 1999; Ricotti 2009).⁴ Third, even as the halo undergoes mergers with other minihalos, the gas in those partner halos may have been unable to cool, as well, owing to the presence of a Lyman-Werner background. Fourth, the seed BH can be kicked out via gravitational recoil from its parent halo, and spend a prolonged period wandering in the lower-density halo outskirts (Blecha & Loeb 2008; TH09; Guedes et al. 2009).

Rather than attempting to model the above effects self-consistently, we simply adopt a fiducial Bondi rate, scaled to the central gas density of the host halo. In an NFW DM halo (Navarro, Frenk & White 1996), the gas density profile has a central core that is proportional to the background IGM gas density (Madau, Ferrara & Rees 2001), $\rho_{\text{gas}}^{(\text{core})} \propto \rho_{\text{gas}}^{(\text{IGM})} \propto (1+z)^3$. Following Ricotti (2009), we assume an isothermal central gas equation of state and adopt the functional form

$$\delta_{\text{core}} = \frac{\rho_{\text{gas}}^{(\text{core})}}{\rho_{\text{gas}}^{(\text{IGM})}} - 1 \approx \Delta_{\text{gas}} \frac{(1 - 0.2\beta/3)(c/0.2)^3}{(c/0.2)^{3(1-0.2\beta/3)} - 0.2\beta/3}. \quad (8)$$

Above, $\Delta_{\text{gas}} \approx 5$ is the mean gas overdensity of the halo; c is the halo concentration parameter; $\beta \equiv c\Gamma/f(c)$ is defined in terms of the parameter $\Gamma = T_{\text{vir}}/T_{\text{IGM}}$ and $f(c) = \ln(1+c) - c/(1+c)$. An important feature of this model is that the core density depends on the IGM temperature (this dependence

⁴ Note that progenitor stars with masses above $40 M_{\odot}$ are expected to collapse directly into a BH and not eject any metals (Heger et al. 2003), eliminating the option of cooling via heavier elements.

arises through the external pressure from the IGM near the halo's virial radius). In the limit of large $\beta \propto T_{\text{vir}}/T_{\text{IGM}}$, $\delta_{\text{core}} \approx 600c^3$. For the concentration parameter, we adopt

$$c = 4.5 \left(\frac{M_{\text{halo}}}{10^6 M_{\odot}} \right)^{-1/8} \left(\frac{1+z}{21} \right)^{-1}, \quad (9)$$

where the normalization and the dependences on M_{halo} and z are based on the simulation results of Bullock et al. (2001) and Wechsler et al. (2002). Several studies have found that the redshift dependence of the concentration parameter weakens at high redshifts $z \gtrsim 4$, and that c has a characteristic minimum value $c_{\text{min}} \sim 3-5$ (Zhao et al. 2003, 2009; Klypin, Trujillo-Gomez & Primack 2011). We impose a conservative lower limit $c \geq 3$ to equation 9; this still allows for the Bondi accretion rate of our BHs to be many orders of magnitude below the Eddington rate.

To summarize, the core gas density is a function of (i) the mean IGM gas density (or redshift), (ii) the halo concentration parameter c , and (iii) the parameter $\Gamma = T_{\text{vir}}/T_{\text{IGM}}$. Given the large uncertainties in modeling the relevant gas density profiles, this Bondi accretion model can be more generally understood in terms of the core overdensity δ_{core} . The critical value of δ_{core} at which $\dot{M}_{\text{Bondi}} = f_{\text{Edd}} \dot{M}_{\text{Edd}}$ is given by

$$\frac{\delta_{\text{crit}}}{f_{\text{Edd}}} \approx 2 \times 10^5 \left(\frac{M_{\text{BH}}}{50 M_{\odot}} \right)^{-1} \left(\frac{T_{\text{vir}}}{400\text{K}} \right)^{3/2} \left(\frac{1+z}{21} \right)^{-3}. \quad (10)$$

2.1.3 Black hole mergers and gravitational recoil

Following the merger of two DM halos that each contain a central BH, we assume that the BHs promptly form a binary and coalesce, aided by the gas surrounding them (e.g. Escala et al. 2004; Cuadra et al. 2009; see Kulkarni & Loeb 2012 for the possible consequences on the high-redshift SMBH population if merger timescales for SMBHs are longer than those for their host halos). A recoil velocity is assigned to the merged binary, with a random value drawn from the fitting formulae given by Lousto et al. (2010), assuming a uniform distribution for the spin magnitudes (in the range $0 < a < 0.93$) and angles with respect to the binary's orbital plane ($0 < \theta < \pi/6$). The latter choice is motivated by Bogdanović, Reynolds & Miller (2007) and Dotti et al. (2009), who have argued that coplanar circumbinary disks can cause moderate spin alignment.

Radial trajectories of the kicked BHs are computed as in TH09, including the effects of dynamical friction and assuming an NFW DM potential superimposed with an isothermal gaseous profile ($\rho_{\text{gas}} \propto r^{-2}$). The latter is taken to be an isothermal cusp in models with an exponential accretion prescription (eq. 5), and the gas profile with a core (eq. 8) for models with the Bondi-limited prescription (eq. 7). Instead of computing the radial trajectories of recoil explicitly for each merger event, we compare the recoil velocity against a retention velocity threshold $v_{\text{ret}}(z, M_{\text{halo}}, M_{\text{BH}})$ which is interpolated from a precompiled table. We consider a recoiling BH to be ejected if it does not return to the halo center on a radial orbit within a Hubble time.

In general, we have found that, somewhat counter-intuitively, the final SMBH mass function at $z \gtrsim 6$ is not highly sensitive to the precise spin prescription (TH09), or

to the central mass distribution of the host galaxy. This is because the recoil velocity is a strongly increasing function of the mass ratio $M_2/M_1 \leq 1$, and the effects of gravitational recoil may be understood rather simply in terms of critical *mass ratios*. Nearly-equal mass BH binaries should almost always be ejected, barring an ultra-massive host halo, strong gas drag from an extremely dense central gas profile, or highly specific, recoil-minimizing BH spin orientations (Haiman 2004). Conversely, mergers with mass ratios $\lesssim 1 : 20$ result in kicks of only $\lesssim 20 - 30 \text{ km s}^{-1}$ regardless of BH spins, and cannot eject BHs from deep inside their halos. Fully-grown SMBHs are ejected only very rarely, as only the most extreme mass ratios and spins can produce kicks large enough to remove them from their massive host halos. Therefore, the spins and the host gravitational potential can influence only the fates of BHs that merge with mass ratios $\sim 1 : 10$ in low-mass halos early on.

In our models, the ancestors of $z \sim 6$ SMBHs tend to be BHs that were sufficiently more massive than their merger partners, and whose mergers occurred in sufficiently massive host halos. The probability that particularly massive BHs survive gravitational recoil events increases with time, as they become successively more massive with respect to their contemporaries and the gravitational potential of their host halos grow deeper (Volonteri & Rees 2006; TH09).

2.2 IGM heating and radiative feedback

2.2.1 (Mini-) quasar emission spectra

We model all accreting black holes as light-bulb (mini-) quasars with Eddington luminosities that are “on” for a fraction $\dot{M}/\dot{M}_{\text{Edd}}$ of the time, and “off” the rest of the time. We assume that a fraction $f_{\text{cor}} = 0.1$ of the total energy is emitted by a hot X-ray corona, modeled as a power-law spectrum above 1 keV with a photon index $\Gamma = 2.0$. The rest of the emission is modeled as a multicolor Shakura-Sunyaev accretion disk (Shakura & Sunyaev 1973), with $\dot{M} = \dot{M}_{\text{Edd}}$ and viscosity parameter $\alpha = 0.1$. We model the spectrum as a one-zone graybody photosphere (Blaes 2004) using the fitting formulae of Tanaka & Menou (2010) for the graybody source function; the disk emission is scaled down by a factor $1 - f_{\text{cor}}$ at all frequencies to accommodate the coronal emission. All miniquasar photons with energies above 13.6 eV are assumed to escape the host halo (Whalen, Abel & Norman 2004).

Figure 1 shows two examples of our model spectra, for miniquasars with $M_{\text{BH}} = 100 M_{\odot}$ and $10^5 M_{\odot}$. For the entire mass range of interest, miniquasars have significant emission above 1 keV (analogous to high-mass X-ray binaries and ultraluminous X-ray sources). Our qualitative findings are robust as long as miniquasars are abundant in the early Universe and are prolific producers of $\sim 1\text{keV}$ X-ray emission (cf. Venkatesan, Giroux & Shull 2001; Madau et al. 2004; Ricotti & Ostriker 2004).

2.2.2 IGM heating and cooling

We treat the IGM as a primordial H+He gas with a mass fraction $Y_{\text{He}} = 0.24$ in He. Initially, it cools adiabatically as

$$T_{\text{IGM}}(z) = 2.73(1+z_t) \left(\frac{1+z}{1+z_t} \right)^2 \text{ K} \approx 9 \left(\frac{1+z}{21} \right)^2 \text{ K}, \quad (11)$$

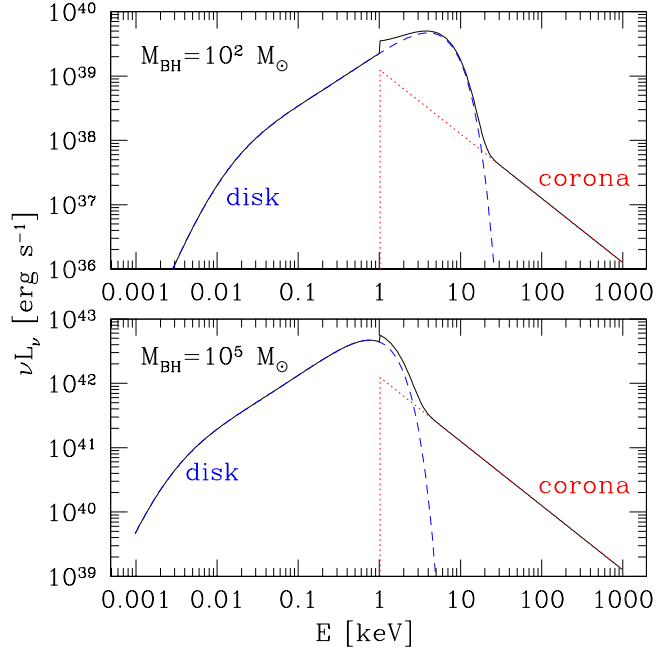


Figure 1. Model spectra of accreting BHs, assumed to be light bulbs radiating at their Eddington luminosity. *Top:* $M_{\text{BH}} = 10^2 M_{\odot}$. *Bottom:* $M_{\text{BH}} = 10^5 M_{\odot}$. The total spectrum (solid black) consists of an α -viscosity accretion disk (dashed blue) and an additional power-law corona at $> 1\text{keV}$ (dotted red).

where $z_t \approx 140$ is the redshift at which the IGM and CMB temperatures decouple (e.g., Peebles 1993).

We follow the temperature and ionization state of the IGM from high to low redshift, together with the evolving BH population, using small timesteps with $\Delta z \approx 0.1$. (At $z > 30$, where miniquasar heating is negligible, we use $\Delta z = 1$.) Across each timestep, the high-energy photons from the accreting BHs heat and ionize the IGM; the conditions in the IGM in turn influence the formation and growth of seed BHs. The ionizing photon background is built up via the cumulative miniquasar emission, with the comoving specific luminosity density

$$\epsilon_{\nu}(z) = \frac{\sum_{\text{BHs}} L_{\nu}(z)}{V}, \quad (12)$$

where $V = 5 \text{ Gpc}^3$ is the comoving volume of our merger-tree simulations. To compute the mean background flux at redshift z , we solve the cosmological radiative transfer equation (Haardt & Madau 1996)

$$j_{\nu}(z) = \frac{1}{4\pi} \int_z^{\infty} \epsilon_{\nu}(z') e^{-\tau_{\nu}(z, z')} \frac{(1+z)^3}{(1+z')^3} c \frac{dt}{dz'} dz', \quad (13)$$

where

$$\tau_{\nu}(z, z') = \int_z^{z'} \sum_j \sigma_{\nu}^j n_0^j (1+z'')^3 c \frac{dt}{dz''} dz'' \quad (14)$$

is the opacity. Above, n_0^j denotes the comoving number density of ion species j (HI, HeI, or HeII), σ_{ν}^j is the photoionization cross section, and $\nu \equiv \nu''(1+z)/(1+z'')$, where ν'' is the emission frequency at redshift z'' .

With the ionization background given by Eq.(13), we follow the thermal evolution of the medium by solving, for

each time-step dt , the energy conservation equation:

$$\frac{du}{dt} = -p \frac{d}{dt} \left(\frac{1}{\rho_{\text{gas}}} \right) - \frac{\Lambda_{\text{net}}}{\rho_{\text{gas}}}, \quad (15)$$

where u , p and ρ_{gas} are the specific internal energy, pressure and density of the gas, respectively, and Λ_{net} is the net heating/cooling rate per unit volume. Heating includes Compton and photoionization heating, while cooling includes line and continuum cooling (and Compton cooling once the IGM temperature rises above T_{CMB}); the first term on the right hand side represents cooling due to adiabatic expansion. The energy equation is solved coupled with the chemistry equations, solving for the abundances of H, H^+ , He, He^+ and He^{++} . The physics of heating and ionization by soft X-ray photons has been described in a number of works (Haardt & Madau 1996; Venkatesan, Giroux & Shull 2001; Furlanetto & Stoever 2010). X-rays propagate to much larger distances than UV photons before being absorbed, photo-ionizing He and H atoms. These photoionizations produce fast photo-electrons, which then partially photoionize the gas through repeated secondary ionizations. We use the recent results by Furlanetto & Stoever (2010) for the fraction of the energy of each fast photo-electron that is used for ionizations and heating. Specifically, we use simple fitting functions to the fractions shown in their Figure 4, and we neglect the dependence on the photoelectron’s energy, which is weak for the relevant range considered here ($E \gtrsim 1\text{keV}$).

3 RESULTS: EFFECT OF IGM HEATING ON BH GROWTH

3.1 SMBH assembly without feedback

To illustrate the overproduction problem, we first show in Figure 2 the SMBH growth history in two reference models without global feedback. The left-hand panels show the results of a model assuming exponential accretion (eq. 4) with $f_{\text{Edd}} = 0.55$; the right panels show a second reference model assuming Bondi-limited accretion (eq. 6) and $f_{\text{Edd}} = 0.8$. In both cases, the BHs do not “know” about the temperature evolution of the IGM. The core gas densities in the Bondi model are computed through eq. 8 as if the IGM cooled adiabatically.

The top panels show the growth of the mass of the most massive BH in the simulation (solid black curves), along with the comoving mass density of all BHs (blue dotted curves) and of only massive BHs with $M > 10^5 M_{\odot}$ (blue dashed curves). The most massive BH is a particularly massive seed with $M_{\text{BH}} \sim 100 M_{\odot}$, left behind by a progenitor star with $M_* \sim 260 M_{\odot}$, just above the pair instability window. Because the most massive SMBHs in our models are products of multiple mergers, their masses scale roughly linearly with the maximum allowed seed mass.

Given that the local SMBH mass density is $\rho_{\text{BH},0} \sim 4 \times 10^5 M_{\odot} \text{Mpc}^{-3}$ (Marconi et al. 2004; Shankar et al. 2004) and that $\gtrsim 90\%$ of this mass density appears to have accreted at $z < 6$ during luminous quasar phases (e.g., Shankar, Weinberg & Miralda-Escudé 2009), the mass density of massive BHs with $M \gtrsim 10^{5-6} M_{\odot}$ at $z \sim 6$ should be at most $\sim \text{few} \times 10^4 M_{\odot} \text{Mpc}^{-3}$. Both models presented in Figure 2 overpredict the global SMBH mass density by sev-

eral orders of magnitude, due to numerous seed BHs growing exponentially near the Eddington rate.

The failure of the Bondi-limited accretion model to avoid this overproduction is not obvious, and is worth explaining in some detail. We find that the seeds surviving their recoil events and producing the $> 10^9 M_{\odot}$ SMBHs at $z = 6$ are those with initial masses of $\sim 30 - 100 M_{\odot}$. As can be seen from equations 8 and 10, these seeds, born in halos with $T_{\text{vir}} \gtrsim 400\text{K}$, quickly get out of their Bondi-phase and switch to the Eddington-limited regime, provided that the central gas density in the halo is sufficiently large (i.e. that the halos have virial temperatures sufficiently above the IGM temperature threshold). As a result, the most massive BHs in the Bondi-limited and the exponential models are similar (compare the black curves in the top left vs. top right panel in Figure 2). As equation 10 shows, the Bondi-limit is important for lower-mass seeds, and it also becomes more important at lower redshifts, where the characteristic densities are lower. This is indeed causes a “dip” and slows down the overall growth of the BH population by accretion in the range $10 \lesssim z \lesssim 20$. In this range, ρ_{BH} is dominated by relatively low-mass ($\lesssim 10^3 M_{\odot}$) BHs, which arise from relatively low-mass seeds, and which suffer prolonged episodes of Bondi-limited accretion. However, as Figure 2 shows, this slow-down is insufficient: the total mass density in $\gtrsim 10^5 M_{\odot}$ BHs by $z \lesssim 10$ is dominated by relatively massive and early-forming seeds, which did not spend a significant time in a Bondi-limited stage.

The bottom panels of Figure 2 show the growth rate $\dot{\rho}_{\text{BH}}$ of the comoving BH mass density (solid black lines), and its three components: creation of new seed BHs (dotted green lines), accretion onto existing seeds (short-dashed blue lines), and ejections due to gravitational recoil (long-dashed red lines). The growth of the total BH density can be broadly divided into two distinct epochs, being dominated by the formation of new seeds at early times ($z \gtrsim 20$) and by accretion at late times ($z \lesssim 15$). The seed formation history is identical in the two models (§2.1.1). In the Bondi-limited case, only BHs with M_{BH} exceeding a critical value M_{crit} (see 10) grow exponentially and the rest accrete at a much lower rate. This leads to a wider distribution in BH masses at late times, which results in fewer BH mergers with comparable masses and thus fewer ejections by gravitational recoil. In the exponential growth model, BHs tend to have similar growth histories; two BHs that have similar masses at a given time will also have similar masses at a later time, unless one grows much more rapidly via mergers. Thus, pairings of BHs of comparable masses are common, resulting in much higher rates of BH ejection. In both models, and generically for assembly models of this type, ejected BHs tend to be somewhat lower-mass BHs residing in lower-mass halos (§2.1.3). As seen in the bottom left panel in Figure 2, the global mass density of nuclear BHs can temporarily *decrease* during phases in which the ejections of low-mass BHs outweigh the sum of accretion onto high-mass BHs and the seed formation rate.

In both accretion models, the growth rate of the overall population $\dot{\rho}_{\text{BH}}$ becomes unrealistically high by $z \sim 9$.⁵ For

⁵ We have checked that despite these high rates, the $z > 6$ SMBHs in our models never consume more than 10 percent of

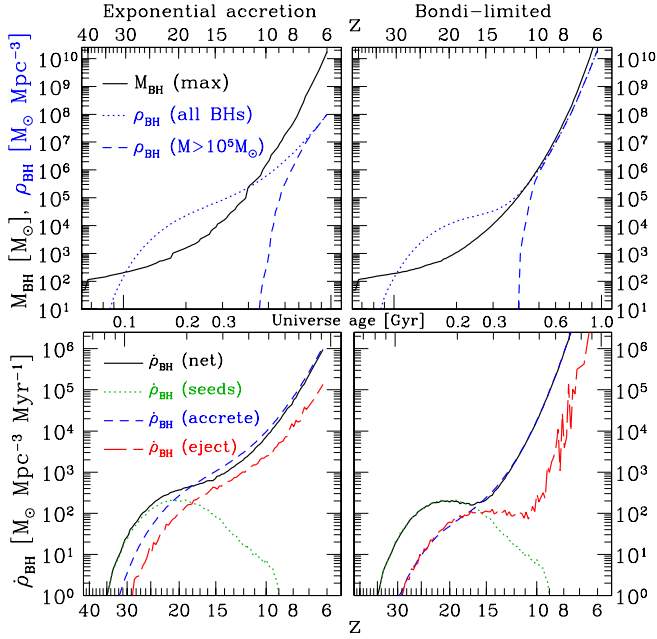


Figure 2. The evolution of the BH population in two models with different accretion prescriptions without global feedback. *Left panels:* All BHs accrete exponentially at a fraction $f_{\text{Edd}} = 0.55$ of the Eddington limit. *Right panels:* Accretion is limited by the local Bondi rate (see text) and by $f_{\text{Edd}} = 0.8$. *Top panels:* The mass of the most massive BH in the simulation (solid black curves), and the comoving density of all BHs (dotted blue) and of only BHs with $M > 10^5 M_{\odot}$ (dashed blue). *Bottom panels:* The growth rate $\dot{\rho}_{\text{BH}}$ of the global BH mass density (solid black), and contributions to it from seed creation (dotted green), gas accretion (short-dashed blue) and recoil-ejections (long-dashed red).

reference, to avoid overproduction, this rate should have a time-averaged value of

$$\langle \dot{\rho}_{\text{BH}}(z > 6) \rangle \lesssim \frac{0.1 \times \rho_{\text{BH},0}}{\Delta t(z > 6)} \sim 60 M_{\odot} \text{Mpc}^{-3} \text{Myr}^{-1}. \quad (16)$$

3.2 SMBH assembly with global IGM warming

The most conspicuous consequence of IGM heating is the inhibition of the gravitational collapse of gas into low-mass halos. The cosmological Jeans mass (e.g., Barkana & Loeb 2001)

$$M_{\text{J}}(z) = \left(\frac{5kT_{\text{IGM}}}{G\mu m_{\text{p}}} \right)^{3/2} \left(\frac{3}{4\pi\rho_{\text{b}}} \right)^{1/2} \quad (17)$$

$$\approx 6.8 \times 10^5 \left(\frac{\mu}{1.2} \right)^{-3/2} \left(\frac{T_{\text{IGM}}}{100\text{K}} \right)^{3/2} \left(\frac{1+z}{21} \right)^{-3/2} M_{\odot}$$

will rise, and gas inside halos whose masses are below this threshold will not collapse to form stars and seed BHs. It has been shown (Gnedin 2000) that the so-called filtering mass, which depends on the temperature history of the IGM, provides a better fit to gas fractions in low-mass halos in numerical simulations than the instantaneous Jeans mass. The

the baryons in a halo. The most massive SMBHs typically have less than one percent of the host halo’s baryon mass.

filtering mass lags the evolution of the Jeans mass, and is therefore lower than the Jeans mass, during the period when the IGM temperature is rising. However, we note that the definition in equation 17 is a factor of 8 lower than the one adopted by Gnedin (2000), and is, in fact, very close to the filtering mass shown in his Figure 3 at the relevant redshifts ($z \gtrsim 10$).⁶ We note that the impact of IGM heating may extend beyond the fiducial Jeans mass: even in a halo above the Jeans mass, gas falls in, at least initially, along a higher adiabat from the pre-heated IGM—this could prevent the gas from condensing to a sufficiently high enough density to activate H_2 cooling. Machacek, Bryan & Abel (2003) and Kuhlen & Madau (2005) both found evidence in 3D simulations that heating the IGM by X-rays can suppress baryonic infall into low-mass halos.

Another consequence of IGM heating may be to suppress the BH accretion rate in pre-existing halos. Machacek, Bryan & Abel (2003) and Kuhlen & Madau (2005) found that an early soft X-ray background can elevate the mean gas temperature inside low-mass minihalos with masses below the collapse threshold. (However, both studies found that the X-ray feedback on cold gas may be *positive* in more massive minihalos; see §4.1 below.) As the IGM heats, the inflow of cool gas into existing halos whose masses fall below the collapse threshold would be suppressed. The heating and evaporation of small halos could in turn impact accretion onto BHs residing in more massive halos, by reducing the amount of cold and dense gas supplied by minor mergers. Furthermore, the accumulating X-ray background can heat the gas inside low-mass halos near or above their virial temperatures, reducing the gas density, or photoevaporating the halo entirely (Shapiro, Iliiev & Raga 2004; Ahn & Shapiro 2007), shutting down Bondi accretion onto the nuclear BH.

There is some circumstantial evidence that the BH accretion rate is tied to the mass supply rate onto the parent halo. Massive BHs appear to have been much more active in the early Universe: most $z \sim 6$ quasars appear to be shining near or slightly above their Eddington luminosities (Willott et al. 2010b), compared to typical Eddington ratios of ~ 0.1 at $z < 4$ (Kollmeier et al. 2006; Kelly et al. 2010). Shankar et al. (2010) concluded that most SMBHs are active as quasars at $z \sim 6$, compared to less than 1% at $z < 2$ (Shankar, Weinberg & Miralda-Escudé 2009). A plausible physical reason behind such hyperactivity is the rapid mass supply to their host halos via mergers with other halos and by accretion; Angulo et al. (2012) observed that numerically simulated host halos of $z \sim 6$ quasars doubled in mass in the preceding 100 Myr.

Motivated by these considerations, we simulate two models of SMBH assembly that include negative feedback due to IGM heating. In both models, the cosmological Jeans mass rises due to IGM heating by miniquasars; new seed BHs are only formed in chemically pristine halos with masses above the Jeans mass. In the first (“exponential”) model, we assume that BHs grow exponentially with $f_{\text{Edd}} = 0.55$

⁶ Naoz & Barkana (2007) showed that the gas density and pressure gradients in the initial conditions after recombination decreases the filtering mass. However, this is below our minimum halo mass imposed by cooling, and does not affect our results.

as in one of the reference models, but that this growth is enabled by the supply of cold gas from the merger-driven growth of the host halo. Thus, we halt BH accretion one e-folding time (≈ 62 Myr, comparable to a typical quasar lifetime; e.g. Martini 2004) after the most recent merger of their host halo with another halo. We additionally require that the merger partner halo exceeds the Jeans mass (so that it contains cold gas). In the second (“Bondi”) model, we assume that BH accretion is instead limited by the Bondi rate in the halo nucleus, which we model as in the second reference model. We again take $f_{\text{Edd}} = 0.8$ and $\rho_{\text{gas}} = \rho_{\text{min}}$. However, the central gas density of the halo depends on the ratio $\Gamma = T_{\text{vir}}/T_{\text{IGM}}$ (eq. 8) – as the miniquasar emission heats the IGM, the core densities in low-mass halos decrease and the Bondi accretion rates of their BHs are suppressed.

3.2.1 Global IGM warming: results

Our results in both the Exponential and the Bondi models are shown in Figure 3. As in Figure 2, the left panels show the exponential accretion model, while the right panels show the Bondi-limited model. The top panels show the growth of the most massive BH in each simulation, along with the global BH mass density ρ_{BH} , while the bottom panels show $\dot{\rho}_{\text{BH}}$ and its components due to seed formation, gas accretion and recoil-ejections. The color and line style schemes are identical to those in Figure 2. For ease of comparison with the reference models, the vertical scales of the graphs are the same as in Figure 2, despite much lower values of $\dot{\rho}_{\text{BH}}$ in the models with feedback.

In the top panels of Figure 4, we show the $z = 6$ BH mass function produced by our models, without (thin lines) and with feedback (thick lines). As with the previous two figures, left panels show the exponential-accretion models and the right panels show the Bondi-limited models. Feedback clearly depresses the late growth of $M_{\text{BH}} \sim 10^{5-7} M_{\odot}$ BHs, while leaving the most massive objects nearly unaffected. Note that the mass function is very steep in the models without feedback. This is because most seeds form within a relatively brief cosmological epoch, and a large number of BHs are allowed to grow at the identical exponential rate.

In the bottom panels of Figure 4, we estimate the luminosity function for the models with feedback that avoid SMBH overproduction. Recall that in order to treat the X-ray emission from accreting BHs, we have approximated them as Eddington-luminosity lightbulbs with a duty cycle $\dot{M}/\dot{M}_{\text{Edd}}$. Using this prescription to translate the mass function into a quasar luminosity function, however, will tend to overestimate quasar luminosities and underestimate their counts (duty cycles). We therefore also consider the opposite extreme estimate for the luminosity function, in which BHs shine at a bolometric luminosity $(\dot{M}/\dot{M}_{\text{Edd}})L_{\text{Edd}}$ and have a duty cycle of 1. The true luminosity function should lie within the bounds set by these two formulations, represented in Figure 4 by the shaded grey region. For reference, we plot the observational determination of the $z \sim 6$ quasar luminosity function (corrected for obscuration) of Willott et al. (2010b; blue dotted lines), as well as the fitting formula suggested by Hopkins, Richards & Hernquist (2007; blue dashed lines).

The luminosity functions predicted by our models, in particular the “exponential” model, may still be too steep

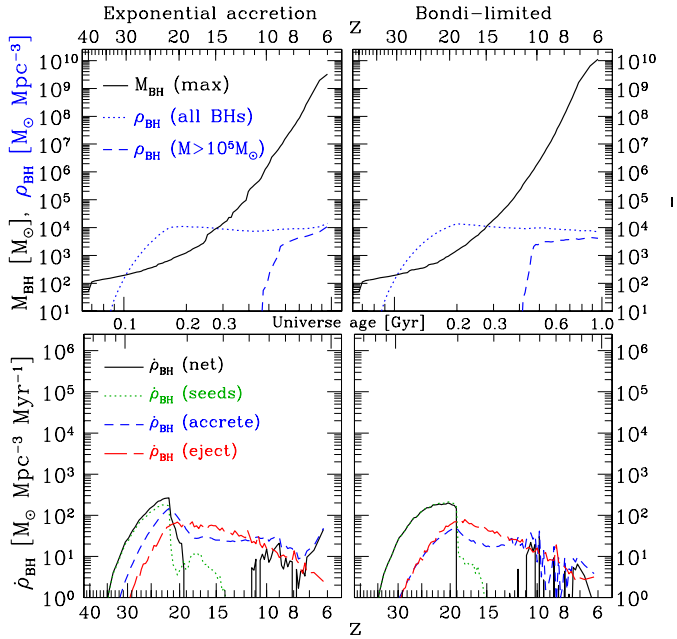


Figure 3. Same as Figure 2, but global IGM heating by accreting BHs suppresses BH formation and growth at late times. *Left panels:* BHs accrete exponentially as in the left panels of Figure 2, but accretion is halted if host halos do not continue merging with massive halos containing cold, collapsed gas. *Right panels:* BH accretion is limited by the local Bondi rate as in the right panels of Figure 2; the rising IGM temperature lowers the halo gas density (eq. 8). In both models, halos below the Jeans mass are disqualified from forming new seed BHs.

below $L \sim 10^{46.5} \text{ erg s}^{-1}$ compared to the best-fit luminosity function of Willott et al. (2010b). However, the faint end of the $z \approx 6$ quasar luminosity function remains highly uncertain. The Willott et al. fit includes a single binned data point below $2 \times 10^{46} \text{ erg s}^{-1}$, and assumes that the fraction of obscured quasars (which is larger for low-luminosity objects; Lawrence 1991) is the same as the one found in the local Universe. The latter point is motivated by the fact that the obscured fraction does not appear to evolve between $z = 0$ and 2 (Ueda et al. 2003), but there has been no direct determination of the obscured fraction at $z \approx 6$.

As Figures 3 and 4 show, both of these models avoid the overproduction of the lower-mass ($M \sim 10^{5-7} M_{\odot}$) BHs, while still producing $M \gtrsim 10^9 M_{\odot}$ by $z \approx 6.4$. Note that the exponential growth model, in which the accretion rate is capped at half of the Eddington limit, falls somewhat short of explaining the $z = 7.08$ quasar SMBH with $M \approx 2 \times 10^9 M_{\odot}$ observed by Mortlock et al. (2011) despite producing a good fit to the $z \approx 6$ mass function of Willott et al. (2010b). At $z = 7.08$, in a simulation volume roughly $1/3$ of the ~ 15 comoving Gpc^3 covered by the UKIDSS, the most massive SMBH in this model is a factor ≈ 4 short. The $z = 7.08$ SMBH can be reproduced with only a slightly higher accretion rate, $f_{\text{Edd}} = 0.6$; however, this overshoots the global mass function and ρ_{BH} by roughly an additional order of magnitude. This illustrates the fact that this SMBH is yet more difficult to accommodate in simple SMBH assembly models. One obvious possibility that the Mortlock et al. SMBH is a mild outlier in

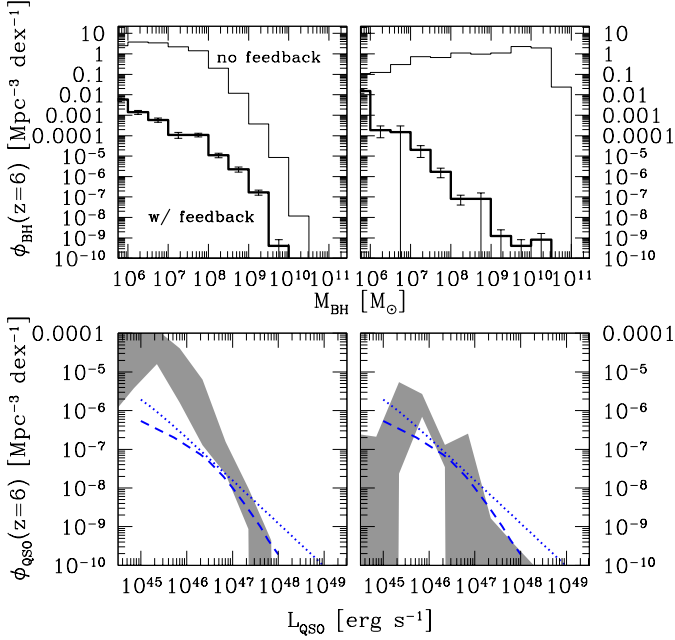


Figure 4. *Top panels:* The $z = 6$ BH mass function in our SMBH assembly models. The thin histograms show the models without feedback, severely overproducing the global SMBH mass density; the thick histograms show the models with feedback. The error bars demarcate the Poisson errors from our simulated sample. *Bottom panels:* The $z = 6$ quasar luminosity function in our models with feedback, shaded in grey between the upper and lower limits for the luminosity and duty cycles of individual BHs (see text). For reference, we show the obscuration-corrected luminosity function found by Willott et al. (2010; blue dashed curve) and the best-fit model for $z = 6$ of Hopkins et al. (2007; blue dotted curve). As with Figs. 2 and 3, the left panels show exponential accretion models with $f_{\text{Edd}} = 0.55$, and the right panels show models where accretion is capped by the Bondi rate and by $f_{\text{Edd}} = 0.8$.

its growth history. While $f_{\text{Edd}} = 0.55$ is a suitable mean value in the context of this model, realistically BHs have a distribution of Eddington ratios and not a single universal value.

In summary, these results of our illustrative models suggest a generic, self-consistent scenario of black-hole-made “climate change”, in which the earliest and most massive accreting BHs heat the IGM and suppress the formation and growth of subsequent generations of BHs. As in the case of global warming on Earth, the negative effects are felt by the next generations: the BHs originally responsible for this feedback are largely unaffected by it, because they reside in the most massive halos that merge frequently with other massive halos and have high central gas densities to facilitate BH growth.

3.2.2 IGM global warming and reionization

We show the thermal and ionization histories of the IGM in Figure 5. As with the previous figures, the exponential accretion models are plotted on the left panels, while the Bondi-limited models are shown on the right. The models with and without feedback are plotted with thick and

thin curves, respectively. Note that in the models without feedback, we still allow miniquasars to heat and ionize the IGM, but BH formation and accretion are assumed to be unaffected by this cosmic climate change. In particular, seed BHs continue to form at $M_{\text{halo}}^{(\text{seed})}$ ($T_{\text{vir}} = 400\text{K}$), and BH accretion rates proceed universally at f_{Edd} in the exponential model, while proceeding as if the IGM were cooling adiabatically in the Bondi model. In the models with feedback, seed formation and accretion are suppressed by the warming of the IGM, as described above in §3.2. The top pair of panels in Figure 5 show the IGM temperature $T_{\text{IGM}}(z)$ for each model. The middle pair show the corresponding cosmological Jeans mass; the seeding mass threshold $M_{\text{halo}}^{(\text{seed})}$ due to H_2 cooling is plotted in blue dashed lines alongside the Jeans mass. The bottom panels show the electron fraction $x_e = (n_{\text{HII}} + n_{\text{HeII}} + 2n_{\text{HeIII}})/(n_{\text{H}} + 2n_{\text{He}})$.

Together, Figures 3 and 5 shed light on the coupling of the BH accretion history with the IGM temperature history. Initially, the evolution of $T_{\text{IGM}}(z)$ and $M_J(z)$ follow a power-law decay due to adiabatic cooling. The buildup of the X-ray background heats the IGM, causing a reduction in the seed BH formation rate once M_J becomes larger than $M_{\text{halo}}^{(\text{seed})}$. The suppression of seed formation occurs at a unique characteristic temperature, which may be estimated analytically as follows. The Jeans mass scales with the IGM temperature and density in the same way that the halo mass scales with the virial temperature and characteristic internal gas density (both require the sound-crossing time to equal the dynamical time): $M \propto (T^3/\rho)^{1/2}$. Accounting for the gas overdensity inside collapsed halos and differences in the conventional normalization coefficients of order unity, this leads to $M_J/M_{\text{halo}} \approx 60(T_{\text{IGM}}/T_{\text{vir}})^{3/2}$, i.e. $M_J \approx M_{\text{halo}}^{(\text{seed})}$ when $T_{\text{IGM}} \approx 26\text{K}$. The rising Jeans mass quenches seed BH formation at $z \approx 18$ for both the exponential model and the Bondi-limited model. At these redshifts, the total nuclear BH mass density is already $\rho_{\text{BH}} \approx 10^4 M_{\odot} \text{Mpc}^{-3}$; however, most ($> 90\%$) of this density still consists of the original seed BHs and there are no holes above $10^4 M_{\odot}$.

We may also understand the energetics of the global IGM warming, as follows. The increase in the IGM thermal energy density, $(3/2)n_b k \Delta T_{\text{IGM}}$ —where n_b is the baryon number density of the IGM and ΔT_{IGM} is the difference between the actual IGM temperature and the value expected from adiabatic cooling (eq. 11)—should scale with the total energy density emitted by accreting BHs. The latter is equal to $\epsilon \Delta \rho_{\text{acc}} c^2$, where $\Delta \rho_{\text{acc}}$ is the global mass density accreted by BHs. Taking into account that only a fraction f_{heat} of the accretion power goes toward heating the IGM, we obtain

$$\Delta T_{\text{IGM}} \approx 10^2 f_{\text{heat}} \frac{\Delta \rho_{\text{acc}}}{M_{\odot} \text{Mpc}^{-3}} \left(\frac{\epsilon}{0.07} \right) \left(\frac{\mu}{1.2} \right) \text{K}. \quad (18)$$

We find that initially, at $z > 20$, only $f_{\text{heat}} \sim 10^{-4} - 10^{-3}$ of the (mini-) quasar energy goes into heating the IGM, but that this increases to 10^{-2} at $z \lesssim 8$. The redshift dependence of the heating efficiency is due to the fact that not all of the hard photons are immediately absorbed by the IGM due to their long mean free paths, which results in a delay between emission and absorption. Further, only 1 – 10% of the spectrum is emitted at $E \sim 1 \text{keV}$, with more massive BHs emitting softer spectra. Some of the energy is also lost to ionization and to the CMB through Compton cooling.

From the accretion history of ρ_{BH} , we can also con-

clude that merely turning off the seed BH formation rate is insufficient to prevent overproduction. This is because X-ray heating is initially inefficient, with only a fraction $f_{\text{heat}} \sim 10^{-4}$ of the BH rest-mass energy at $z \sim 20$ going into elevating the gas temperature. The global BH density must therefore grow to a value as large as $10^4 \text{ M}_\odot \text{ Mpc}^{-3}$ for global X-ray feedback to halt seed BH formation (at $T_{\text{IGM}} \gtrsim 30\text{K}$). At the redshifts where this occurs ($z \sim 20$), the most massive BHs are at most $\sim 10^3 \text{ M}_\odot$. If all BHs were to grow exponentially from this point onward, by the time the most massive BHs reach 10^9 M_\odot , the entire population must grow by similar factors of $\sim 10^6$. Even allowing for some of the BH growth to occur via mergers, extreme overproduction of ρ_{BH} is inevitable. To prevent overproduction, either another mechanism must regulate (much more severely) the formation of seed BHs, or BH accretion must be (preferentially) extremely inefficient inside in low-mass halos at later times.

In both models with feedback, the BH accretion rate is indeed reduced preferentially inside low-mass halos. In the exponential accretion model, BH growth is reduced in host halos that do not continue merging with other halos that exceed the Jeans mass. (Note that this suppression kicks in at $z \approx 25$, before seed BH formation rates are affected.) In the Bondi-limited model, IGM heating lowers the central halo gas densities, and the corresponding Bondi rate, in the lower-mass halos.

Unsurprisingly, the same growth models without feedback that overproduce the massive BH population also appear to overpredict its contribution to reionization. Current observational constraints indicate that reionization was still ongoing at $z \gtrsim 7$ (e.g. Fan, Carilli & Keating 2006), and that the optical depth of the IGM to Thomson scattering is $\tau_{\text{es}} = 0.088 \pm 0.014$, only about half of which is accounted for by fully ionized gas between $0 < z < 6$ (CMB measurements; Komatsu et al. 2011). Our “exponential” model without feedback reionizes the Universe by $z_r = 8.4$ and predicts an IGM Thomson optical depth of $\tau_{\text{es}} \approx 0.09$, while our “Bondi” model without feedback completes reionization by $z_r = 9.1$ and predicts $\tau_{\text{es}} \approx 0.11$. These models reionize the Universe earlier than the empirical constraints, *despite neglecting contributions to reionization by the stellar UV radiation accompanying the mini-quasars BHs*. The models with feedback, on the other hand, fall well short of the empirical constraints (neither completes reionization by $z = 6$) and allow room for stars to be the primary sources of reionization. Dijkstra, Haiman & Loeb (2004) showed that even scenarios where the contribution to reionization by miniquasars is $\sim 10 - 20\%$ are consistent with the observed unresolved soft X-ray background near $1 - 2 \text{ keV}$. As our models with miniquasar feedback have lower contributions to reionization (and also because our miniquasar spectra are softer than the one used by those authors), we conclude that they are well within the empirical constraints on the X-ray background (see, e.g., Dijkstra et al. 2012, for a recent study).

3.2.3 BH merger rates

In Figure 6, we show the number of BH mergers at $z > 6$ in the binary mass window $10^4 \text{ M}_\odot < M(1+z) < 10^7 \text{ M}_\odot$, the estimated sensitivity window for major mergers

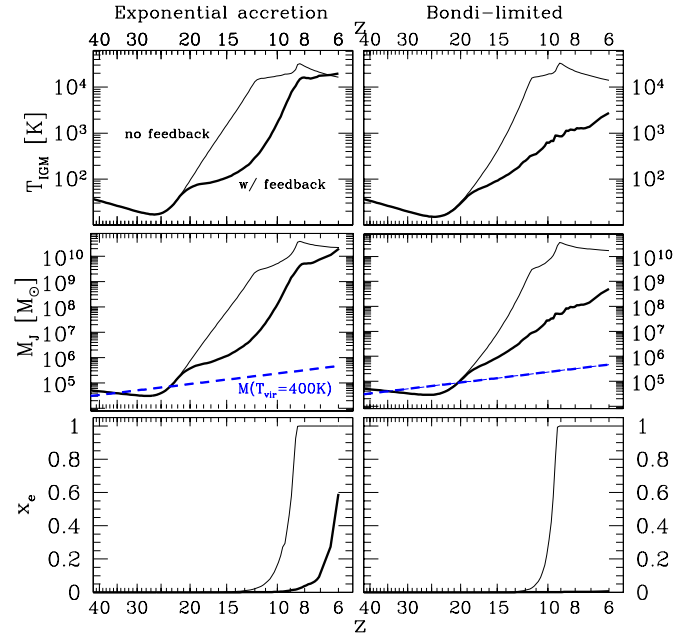


Figure 5. *Top panels:* The IGM temperature as a function of redshift. *Middle:* The cosmological Jeans mass (black solid curves) and our fiducial halo mass threshold for seed BH formation (dashed blue curves). *Bottom:* The IGM electron fraction. Thin curves represent models without feedback, whose BH mass evolution is given in Fig. 2; thick curves represent the models with feedback shown in Fig. 3. As in Figs. 2–4, the exponential accretion models are shown on the left and the Bondi-limited models on the right.

for the proposed gravitational-wave detector *eLISA*/NGO (Amaro-Seoane et al. 2012). The merger rates are shown in our two feedback models, in the previous figures. Both models predict that ≈ 30 major mergers (binary mass ratios $0.1 < q \leq 1$) per year per unit redshift may be detectable at $6 < z < 10$, with approximately twice as many events with mass ratios $q > 0.01$. TH09 found that in a class of simplified models that prevent overproduction by requiring that the $z > 6$ quasar SMBHs form from extremely rare seeds, the detection rate may be zero over the mission lifetime. It is encouraging that in the new models presented here, the seeds are systematically common and the detection rates are nonzero (see explanation for this difference below).

The majority of mergers occur with mass ratios $0.01 \leq q \leq 0.1$ (see also Holley-Bockelmann et al. 2010). Mergers with more nearly equal masses are relatively rare, because (i) feedback tends to increase the mass discrepancy of BH pairs by preferentially suppressing the growth of lower-mass BHs, (ii) BHs that survive recoil events tend to become increasingly more massive with respect to their contemporaries, as explained above, and (iii) halos with very different masses are considered unable to coalesce in our merger tree, due to the long merger timescales (see TH09 for details).

3.2.4 Effects of the Lyman-Werner background

We have also run models that included a global Lyman-Werner (LW) background produced by the progenitor stars of the seed BHs, which can raise the minimum halo mass

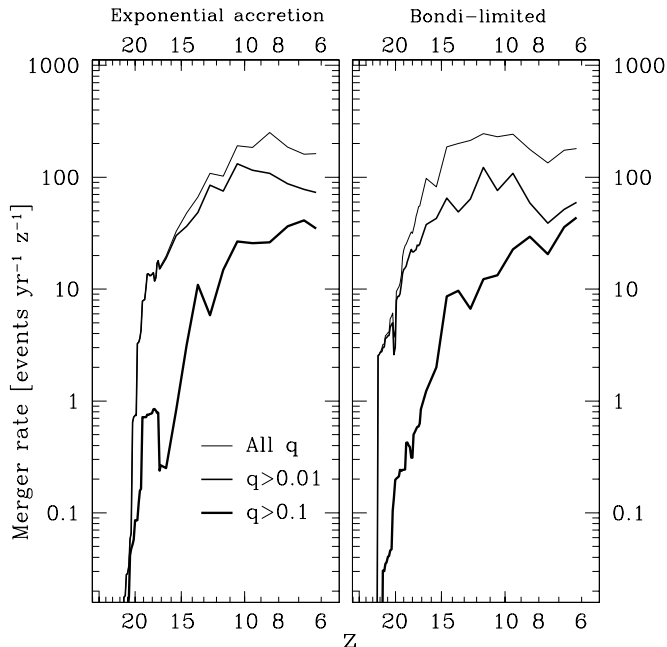


Figure 6. BH merger rates for the two assembly models with feedback in the approximate detection window of the proposed detector *eLISA*/NGO, binary mass $10^4 M_\odot < M(1+z) < 10^7 M_\odot$. The line styles demarcate the binary BH mass ratio $q \leq 1$; in order of increasing thickness: any $q > 0$, $q \geq 0.01$, and $q \geq 0.1$.

threshold for subsequent seed formation. This background and the associated mass threshold can be calculated as follows. Approximately 10^4 photons with energies $E \approx 12.9$ eV are produced per baryon of a progenitor star. Through our Salpeter mass function and our progenitor-to-seed mass relation (eq. 3), the comoving mass density of progenitors is related to that of the seeds as $\rho_{\text{PopIII}} \approx 3.91 \times \int_0^\infty \dot{\rho}_{\text{creat}}(z) dz$. The fraction of the photon energy that contributes to the background, after radiative transfer, is $\lesssim 1/10$ (Haiman, Rees & Loeb 1997; Haiman, Abel & Rees 2000). This gives a characteristic early LW background intensity of

$$J_{\text{LW}} \approx 6 \times 10^{-23} \left(\frac{\rho_{\text{PopIII}}}{10^4 M_\odot \text{Mpc}^{-3}} \right) \left(\frac{1+z}{21} \right)^3 \times \text{erg s}^{-1} \text{cm}^{-2} \text{Hz}^{-1} \text{sr}^{-1}. \quad (19)$$

Using the fitting formula from the simulations of Machacek, Bryan & Abel (2001), this leads to a minimum halo mass scale for subsequent seed formation:

$$M_{\text{LW}} \approx 2 \times 10^5 \left(\frac{\rho_{\text{PopIII}}}{10^4 M_\odot \text{Mpc}^{-3}} \right)^{1/3} \left(\frac{1+z}{21} \right)^{-1/2} M_\odot. \quad (20)$$

In our simulations, this mass scale is only a factor of a few above the fiducial $T_{\text{vir}} = 400\text{K}$ threshold (eq. 2) during the brief interval $20 \lesssim z \lesssim 25$, before the X-ray global warming abruptly turns off seed formation (Fig. 3).

The net effect of the LW background was negligible in the runs that included both LW and X-ray feedback. As such, and given the order-unity errors associated with LW radiative transfer (“sawtooth” modulation; see Haiman et al. references above) and in the merger tree itself, we have

shown above only the results with the X-ray feedback to best highlight the effects of the latter.

The above calculation may underestimate the early LW background, as it does not account for the possibility of PopIII seeds forming in groups alongside the progenitors of the BH seeds. At later times, halos with virial temperatures above 10^4K will efficiently form stars and add to the LW background; however, this occurs long after the X-rays have turned off seed formation. Even if the LW background is much higher than what we have estimated here, it still may not suppress BH accretion inside previously seeded halos, due to self-shielding (Draine & Bertoldi 1996; cf. Wolcott-Green, Haiman & Bryan 2011 and refs. therein).

4 DISCUSSION

4.1 Comparison to Other Work

X-ray heating and early reionization by miniquasars has been studied by a number of authors. The broader effects of various high- z X-ray backgrounds was surveyed by Oh (2001) and Venkatesan, Giroux & Shull (2001), with a special emphasis on the temperature and ionization structure of the IGM before reionization is complete. Machacek, Bryan & Abel (2003) used numerical simulations to study the effects of an early soft X-ray background on the temperature and density of gas inside minihalos at $20 \lesssim z \lesssim 30$. At these redshifts, the $1 - 2$ keV flux in our models is comparable to their parameter choices $\epsilon_X = 1$ and $\epsilon_X = 10$, and their results are consistent with what we find at the onset of feedback in our models. They report that X-ray heating results in a moderate reduction (by a factor of a few) of the cold gas fraction in minihalos with $M_{\text{halo}} \lesssim 10^6 M_\odot$, a mass range comparable to the heating-elevated Jeans mass in our models. They also found that the mean gas temperature inside less massive halos with $M_{\text{halo}} \lesssim 10^5 M_\odot$ can be elevated by an order of magnitude, consistent with our assumption that an X-ray background can act to suppress BH accretion in halos with $M_{\text{halo}} \lesssim M_J$.

Madau et al. (2004) made a first attempt at specifically treating the impact of the first BHs on the global IGM in more detail, but did not explicitly include feedback by X-ray heating on the later generations of BHs. Ricotti & Ostriker (2004) developed a similar semi-analytical model for early “pre-ionization” by seed BHs, with the aim of identifying a BH growth scenario which could account for the large Thomson-scattering optical depth inferred by the earlier CMB measurements. Their study, while including the effect of IGM heating on suppressing virialization below the Jeans mass, did not investigate the corresponding modification of the resulting BH mass function. Ricotti, Ostriker & Gnedin (2005) studied X-ray pre-ionization by means of cosmological simulations. However, their focus was again on the observational signatures in the CMB and 21-cm signal, rather than on the growth of SMBHs.

More recently, Devecchi et al. (2012) explored the formation of nuclear star clusters and BH seeds, tracking the chemical, radiative and mechanical feedback of stars on the baryonic component of the evolving halos. In particular, they examined the role of the LW photons in suppressing star formation, but did not include the rise

of the Jeans mass due to X-ray heating of the IGM by the seeds BHs. Feedback effects from the LW photons in shaping BH growth in the most massive ($10^{12-13}M_{\odot}$) halos at $z = 6$ have also been recently examined in detail by Petri, Ferrara & Salvaterra (2012) and Agarwal et al. (2012), using merger trees and N-body simulations, respectively; however, those studies did not examine feedback on the lower-mass BHs in smaller halos. In principle, LW radiation could help alleviate the SMBH overprediction problem, by disabling the cooling in low-mass halos at very early times (Haiman & Bryan 2006) - this is similar to the X-ray background, although likely restricted to lower-mass minihalos (e.g., Machacek, Bryan & Abel 2001).

Finally, X-rays from miniquasars can also exert positive feedback by triggering the formation of molecular hydrogen (Haiman, Abel & Rees 2000; Machacek, Bryan & Abel 2003; Kuhlen & Madau 2005; Jeon et al. 2012). For example, Machacek, Bryan & Abel (2003), Kuhlen & Madau (2005) and Jeon et al. (2012) found that the X-rays can *increase* the amount of cold and dense gas (and thus star formation) in the cores of massive minihalos in their simulations. This runs contrary to the assumption in our “Bondi-limited” model that X-rays cause a warming of the cores of low-mass halos.⁷ However, the results of Kuhlen & Madau (2005) suggest that at sufficiently high X-ray fluxes, the heating outweighs the enhanced H_2 cooling and the feedback on the cold gas density becomes negative. The value of the X-ray flux where this turnover occurs in their simulation—in minihalos in close proximity of their miniquasar; $\epsilon_X \sim$ a few at ~ 1 keV in the normalization convention of Machacek, Bryan & Abel (2003)—is reached in our models at $z \sim 25 - 20$ when $\rho_{\text{BH}} \gtrsim 10^3 M_{\odot} \text{ Mpc}^{-3}$, and exceeded soon thereafter. This suggests that the X-ray background fluxes in our models are large enough to induce negative feedback. Furthermore, the $E \gtrsim 1$ keV X-rays have mean free paths of ~ 1 Gpc. The simulation volumes of $\sim 1 \text{ Mpc}^3$ employed by Kuhlen & Madau (2005) and Jeon et al. (2012) do not account for the X-rays originating from sources outside the box and thus do not address the early buildup of a global X-ray background. (Kuhlen & Madau 2005 turn on a single miniquasar at $z = 21$.) Finally, even if the X-rays exert a positive feedback by increasing the H_2 cooling, the net effect may also be negative in the presence of a strong LW field accompanying the X-rays. Whether, and to what degree, X-rays can induce positive feedback on structure formation and early BH growth remains very much an open question.

4.2 General Comments on Viable SMBH Growth Scenarios

The puzzle of the origins of the $z \approx 6 - 7$ quasar SMBHs has motivated numerous recent theoretical investigations. Here,

⁷ If the bottleneck on BH accretion is not the central cold gas density but rather the external supply of gas, then the X-ray-induced suppression of baryonic infall found by Machacek, Bryan & Abel (2003), Kuhlen & Madau (2005) and others should lead to a negative feedback on BH growth, as assumed in our “exponential growth” model.

remark on possible SMBH assembly models, attempting to generalize the results we obtained above.

4.2.1 Explaining the monsters

First, what is necessary to explain the individual SMBHs? We find that for the most massive BHs in our simulations to grow to $M \sim 10^9 M_{\odot}$ by $z \approx 7$ (i.e., to explain the Mortlock et al. (2011) quasar observation), a seed BH left behind by a PopIII star and starting at $100 M_{\odot}$ at $z \approx 40$ must have an effective e-folding time of $\lesssim 55$ Myr. That is, the mean Eddington ratio must be $f_{\text{Edd}} \gtrsim 0.6$ for radiative efficiency $\epsilon = 0.07$. Or, more generally, these two quantities must satisfy $f_{\text{Edd}}(1 - \epsilon)/\epsilon \gtrsim 8$. As the elapsed time between $z \approx 40$ and $z \approx 7.08$ is ≈ 700 Myr, this lower limit corresponds to accretion-driven growth by a factor of a few $\times 10^5$. Our models show that mergers can contribute to assembly by an additional factor 10 – 100. Note that for the progenitors of the $z \sim 6$ quasar SMBHs, this requires that the mean accretion be close to 1, that the radiative efficiency be no larger than ~ 0.1 , or both. Note that the above requirement suggests that the progenitors of the $z > 6$ quasar SMBHs have (averaged over their growth histories) accretion rates close to or exceeding the Eddington limit, relatively low radiative efficiencies $\epsilon \lesssim 0.1$, or both. Such low radiative efficiencies suggest that the BHs cannot be spinning rapidly, consistent with accretion disk models with magnetohydrodynamic turbulence (see, e.g. Shapiro 2005, and references therein). A hypothetical, single BH accreting at the Eddington limit and $\epsilon = 0.07$ can grow by a factor $\approx 10^9$ in the same redshift interval.

Another possibility is that the ancestors of the monster SMBHs were born with much higher masses. For example, particularly massive BHs with $M_{\text{BH}} > 10^4 M_{\odot}$ could have formed in halos whose gaseous components have unusually low angular momentum (Koushiappas, Bullock & Dekel 2004; Lodato & Natarajan 2006); in halos that are heavily irradiated by massive neighbors (Dijkstra et al. 2008); in environments with high ambient magnetic fields (Sethi, Haiman & Pandey 2010); or in rare instances of ionizing shocks in dense halo cores (Inayoshi & Omukai 2012).

A common minimum requirement for both classes of seed models is that a $\sim 10^5 M_{\odot}$ BH be in place by $z \approx 10$; such BHs can grow at the Eddington rate to $\sim 10^9 M_{\odot}$ by $z \approx 7$. The recent work by Di Matteo et al. (2012) suggests that once such a BH is in place, then cold gas accretion by the rapidly growing host halo could help deliver the gas, at least on large scales, to sustain its near-Eddington growth. Any seed model that satisfies this condition can, in principle, explain the individual quasar SMBH masses observed to date. The above requirement also suggest a fundamental degeneracy for assembly models of high-redshift SMBHs in the $6 \lesssim z \lesssim 10$ range.

4.2.2 Modeling the overall population

In light of the above points, the greater challenge arguably lies in distinguishing between the various assembly scenarios. Probing the non-degenerate parameter space ($M_{\text{BH}} < 10^5 M_{\odot}, z \gtrsim 10$) through direct electromagnetic observation will be difficult. This is about the detection

sensitivity of the *James Webb Space Telescope*, assuming Eddington luminosity and a $\sim 10^5$ s integration (Haiman 2012). If IGM preheating suppresses star formation in halos with $M_{\text{halo}} \lesssim 10^9 M_{\odot}$, this may lead to an observable faint-end cutoff in the high-redshift galaxy luminosity function (Barkana & Loeb 2000) and a drop in the rate of high-redshift supernovae (Mesinger, Johnson & Haiman 2006); both effects could be observed by the *JWST* and provide circumstantial evidence for negative feedback on low-mass halos. However, the most obvious candidate for distinguishing models is a gravitational-wave detector such as *eLISA/NGO*, which could directly constrain BH merger rates, masses and abundances at high-redshift.

Previous studies had suggested that to avoid overproduction, seed BHs must be rare (Bromley, Somerville & Fabian 2004; TH09). In principle, the occupation fraction of SMBHs in galaxies can approach unity by low redshift even if nuclear BHs were very rare at early times (Menou, Haiman & Narayanan 2001; Lippai, Frei & Haiman 2009). If seeds are indeed rare, then it is conceivable that the BH merger rate at high redshift ($z \gtrsim 6$) would be so low that no detectable events will be expected by *eLISA/NGO* (TH09). A rare seed BH population would also have a smaller impact via global feedback. Therefore, one way to indirectly confirm such models is by ruling out alternative scenarios, with common seed BHs, through null detections.

The alternative possibility proposed here is that seeds are systematically much more common, but that BHs grow much less rapidly in low-mass halos at late times. This could be because AGN feedback or other local processes self-regulate the BH mass with respect to the host galaxy properties, i.e. processes similar to those resulting in the locally observed $M - \sigma$ relation (TH09, Volonteri & Natarajan 2009). In this paper, we have shown that similar effects can be produced instead by global feedback; the hard photons from the early accreting BHs can heat the IGM and regulate subsequent BH formation and growth. The same BHs that go on to assemble the $z \sim 6$ SMBHs can slow the growth of the low end of the BH mass function and avoid overproduction. One important consequence of the common-seed scenarios, regardless of whether the mechanism regulating BH growth is local or global, is that the mergers of the SMBH ancestors and their intermediate-mass contemporaries should be frequent enough to be detectable by an observatory such as *eLISA/NGO* (cf. Sesana, Volonteri & Haardt 2007, Micic et al. 2007).

Additionally, if the seeds are common, then the X-rays emitted in the course of their mass growth could generically influence cosmological structures. This may be inevitable, regardless of whether the first nuclear BHs had masses of $10 M_{\odot}$ or $10^5 M_{\odot}$; en route to becoming $10^{7-9} M_{\odot}$ SMBHs, the vast majority of the mass growth must occur through accretion. Indeed, 18 suggests that the IGM will be heated to $\sim 10^4$ K if the comoving SMBH mass density at $z = 6$ is several percent of the present-day value, and if $\sim 0.1\%$ of the miniquasar energy output required to build up this mass density goes toward heating the IGM.

Our models predict that miniquasars play a significant role in establishing the cosmological temperature history of the IGM, since X-rays from miniquasars would heat the early Universe much more effectively

than UV radiation from PopIII stars (Madau et al. 2004; Ciardi, Salvaterra & Di Matteo 2010). Our results suggest that PopIII star formation may be affected by miniquasars as early as $z \approx 20$. Other sources, such as LW radiation from PopIII stars and the accreting BHs, hard photons from non-nuclear stellar-mass BHs (Wheeler & Johnson 2011) and high-mass X-ray binaries (Mirabel et al. 2011), or local AGN feedback and regulation, may also have contributed to this feedback.

5 CONCLUSIONS

Observations of high-redshift quasars at $z \gtrsim 6$ imply that SMBHs with masses $M \gtrsim 10^9 M_{\odot}$ were in place as early as $z > 7$. In this paper, we considered models in which these SMBHs grow from stellar-mass seed BHs forming at ultra-high redshifts (i.e. the remnants of first-generation stars at $z \sim 30 - 40$), obeying the Eddington limit on the mass accretion rate. Previous work has shown that this is feasible, but only if the duty cycle for accretion is of order unity.

Here we highlighted a relatively under-appreciated problem in this class of models: unless the growth of BHs in low-mass halos is preferentially and severely suppressed, the models overpredict the abundance of $10^{5-7} M_{\odot}$ BHs in galactic nuclei by several orders of magnitude.

Using Monte-Carlo realizations of the merger and growth history of BHs, we show that the X-rays emitted by the earliest accreting BHs can heat the IGM, and suppress the formation and growth of subsequent generations of BHs in low-mass halos. In this “global warming” scenario, the BHs originally responsible for the warming are largely unaffected by it, because they reside in the most massive halos, well above the Jeans mass, and frequently merge with other massive halos with cold gas, facilitating BH growth. However, the negative effects are felt by the next generations of low-mass halos, in which seed formation and BH accretion are suppressed.

We presented specific models with global miniquasar feedback that provide excellent agreement with recent estimates of the $z = 6$ SMBH mass function. These models could be constrained through direct observations by *JWST*, and through the detection of tens of BH mergers at $z > 6$ by the proposed gravitational-wave observatory *eLISA/NGO*.

We compared our work to previous studies investigating the effects of X-ray feedback on early structure formation. A primary uncertainty is whether, and to what degree, a moderate X-ray background may induce *positive* feedback on the cold gas content of minihalos through enhanced H_2 formation and cooling, and whether this effect outweighs the heating of the gas by the X-rays. Finally, a limitation of our merger tree approach is that we do not consider local effects due to clustering and to proximity to miniquasars, which may be significant (e.g., Kuhlen & Madau 2005). While our work serves as a proof-of-concept that global X-ray feedback from accreting BHs can regulate their growth, more detailed studies on this subject are warranted.

ACKNOWLEDGMENTS

We thank Jerry Ostriker and Greg Bryan for insightful conversations, and Daniel Mortlock for useful discussions about the $z = 7.08$ quasar. RP and ZH thank the Centro de Ciencias de Benasque Pedro Pascual, where this project was initiated. This work was partially supported by NSF grant AST-1009396 (to RP) and by NASA grant NNX11AE05G (to ZH).

REFERENCES

- Abel T., Bryan G. L., Norman M. L., 2002, *Science*, 295, 93
- Agarwal B., Khochfar S., Johnson J. L., Neistein E., Dalla Vecchia C., Livio M., 2012, arXiv e-prints 1205.6464
- Ahn K., Shapiro P. R., 2007, *MNRAS*, 375, 881
- Alvarez M. A., Wise J. H., Abel T., 2009, *ApJ*, 701, L133
- Amaro-Seoane P. et al., 2012, arXiv e-prints 1201.3621
- Angulo R. E., Springel V., White S. D. M., Cole S., Jenkins A., Baugh C. M., Frenk C. S., 2012, arXiv e-prints 1203.5339
- Barkana R., Loeb A., 2000, *ApJ*, 539, 20
- , 2001, *Physics Reports*, 349, 125
- Begelman M. C., Volonteri M., Rees M. J., 2006, *MNRAS*, 370, 289
- Blaes O. M., 2004, in *Accretion Discs, Jets and High Energy Phenomena in Astrophysics*, V. Beskin, G. Henri, F. Menard, G. Pelletier, J. Dalibard, ed., Springer Publishing Company, New York, NY, USA, pp. 137–185
- Blecha L., Loeb A., 2008, *MNRAS*, 390, 1311
- Bogdanović T., Reynolds C. S., Miller M. C., 2007, *ApJ*, 661, L147
- Bond J. R., Arnett W. D., Carr B. J., 1984, *ApJ*, 280, 825
- Bromley J. M., Somerville R. S., Fabian A. C., 2004, *MNRAS*, 350, 456
- Bromm V., Coppi P. S., Larson R. B., 2002, *ApJ*, 564, 23
- Bromm V., Loeb A., 2003, *ApJ*, 596, 34
- Bullock J. S., Kolatt T. S., Sigad Y., Somerville R. S., Kravtsov A. V., Klypin A. A., Primack J. R., Dekel A., 2001, *MNRAS*, 321, 559
- Ciardi B., Salvaterra R., Di Matteo T., 2010, *MNRAS*, 401, 2635
- Ciotti L., Ostriker J. P., 2001, *ApJ*, 551, 131
- Cuadra J., Armitage P. J., Alexander R. D., Begelman M. C., 2009, *MNRAS*, 393, 1423
- Devecchi B., Volonteri M., 2009, *ApJ*, 694, 302
- Devecchi B., Volonteri M., Rossi E. M., Colpi M., Portegies Zwart S., 2012, *MNRAS*, 421, 1465
- Di Matteo T., Khandai N., DeGraf C., Feng Y., Croft R. A. C., Lopez J., Springel V., 2012, *ApJ*, 745, L29
- Dijkstra M., Gilfanov M., Loeb A., Sunyaev R., 2012, *MNRAS*, 421, 213
- Dijkstra M., Haiman Z., Loeb A., 2004, *ApJ*, 613, 646
- Dijkstra M., Haiman Z., Mesinger A., Wyithe J. S. B., 2008, *MNRAS*, 391, 1961
- Dotti M., Montuori C., Decarli R., Volonteri M., Colpi M., Haardt F., 2009, *MNRAS*, 398, L73
- Draine B. T., Bertoldi F., 1996, *ApJ*, 468, 269
- Escala A., Larson R. B., Coppi P. S., Mardones D., 2004, *ApJ*, 607, 765
- Fan X., 2006, *New Astron. Rev.*, 50, 665
- Fan X., Carilli C. L., Keating B., 2006, *ARAA*, 44, 415
- Furlanetto S. R., Stoever S. J., 2010, *MNRAS*, 404, 1869
- Gnedin N. Y., 2000, *ApJ*, 542, 535
- Greif T. H., Bromm V., Clark P. C., Glover S. C. O., Smith R. J., Klessen R. S., Yoshida N., Springel V., 2012, *MNRAS*, 424, 399
- Greif T. H., White S. D. M., Klessen R. S., Springel V., 2011a, *ApJ*, 736, 147
- Greif T. H., Springel V., White S. D. M., Glover S. C. O., Clark P. C., Smith R. J., Klessen R. S., Bromm V., 2011b, *ApJ*, 737, 75
- Guedes J., Madau P., Kuhlen M., Diemand J., Zemp M., 2009, *ApJ*, 702, 890
- Haardt F., Madau P., 1996, *ApJ*, 461, 20
- Haehnelt M. G., 2003, *Class. Quantum Gravity*, 20, 31
- Haehnelt M. G., Rees M. J., 1993, *MNRAS*, 263, 168
- Haiman Z., 2004, *ApJ*, 613, 36
- , 2012, arXiv e-prints 1203.6075
- Haiman Z., Abel T., Rees M. J., 2000, *ApJ*, 534, 11
- Haiman Z., Bryan G. L., 2006, *ApJ*, 650, 7
- Haiman Z., Loeb A., 2001, *ApJ*, 552, 459
- Haiman Z., Rees M. J., Loeb A., 1997, *ApJ*, 476, 458
- Haiman Z., Thoul A. A., Loeb A., 1996, *ApJ*, 464, 523
- Heger A., Fryer C. L., Woosley S. E., Langer N., Hartmann D. H., 2003, *ApJ*, 591, 288
- Holley-Bockelmann K., Micic M., Sigurdsson S., Rubbo L. J., 2010, *ApJ*, 713, 1016
- Hopkins P. F., Richards G. T., Hernquist L., 2007, *ApJ*, 654, 731
- Hosokawa T., Omukai K., Yorke H. W., 2012, arXiv e-prints 1203.2613
- Hosokawa T., Omukai K., Yoshida N., Yorke H. W., 2011, *Science*, 334, 1250
- Inayoshi K., Omukai K., 2012, *MNRAS*, 422, 2539
- Jarosik N. et al., 2011, *ApJS*, 192, 14
- Jeon M., Pawlik A. H., Greif T. H., Glover S. C. O., Bromm V., Milosavljević M., Klessen R. S., 2012, *ApJ*, 754, 34
- Kelly B. C., Vestergaard M., Fan X., Hopkins P., Hernquist L., Siemiginowska A., 2010, *ApJ*, 719, 1315
- Klypin A. A., Trujillo-Gomez S., Primack J., 2011, *ApJ*, 740, 102
- Kollmeier J. A. et al., 2006, *ApJ*, 648, 128
- Komatsu E. et al., 2011, *ApJS*, 192, 18
- Koushiappas S. M., Bullock J. S., Dekel A., 2004, *MNRAS*, 354, 292
- Kramer R. H., Haiman Z., Oh S. P., 2006, *ApJ*, 649, 570
- Kuhlen M., Madau P., 2005, *MNRAS*, 363, 1069
- Kulkarni G., Loeb A., 2012, *MNRAS*, 422, 1306
- Lacey C., Cole S., 1993, *MNRAS*, 262, 627
- Lawrence A., 1991, *MNRAS*, 252, 586
- Lippai Z., Frei Z., Haiman Z., 2009, *ApJ*, 701, 360
- Lodato G., Natarajan P., 2006, *MNRAS*, 371, 1813
- Loeb A., Rasio F. A., 1994, *ApJ*, 432, 52
- Lousto C. O., Campanelli M., Zlochower Y., Nakano H., 2010, *Class. Quantum Gravity*, 27, 114006
- Machacek M. E., Bryan G. L., Abel T., 2001, *ApJ*, 548, 509
- , 2003, *MNRAS*, 338, 273
- Madau P., Ferrara A., Rees M. J., 2001, *ApJ*, 555, 92
- Madau P., Rees M. J., Volonteri M., Haardt F., Oh S. P., 2004, *ApJ*, 604, 484

- Marconi A., Risaliti G., Gilli R., Hunt L. K., Maiolino R., Salvati M., 2004, *MNRAS*, 351, 169
- Martini P., 2004, in *Coevolution of Black Holes and Galaxies*, L. C. Ho, ed., Cambridge University Press, Cambridge, United Kingdom, pp. 169–+
- Menou K., Haiman Z., Narayanan V. K., 2001, *ApJ*, 558, 535
- Merloni A., Heinz S., 2008, *MNRAS*, 388, 1011
- Mesinger A., Johnson B. D., Haiman Z., 2006, *ApJ*, 637, 80
- Micic M., Holley-Bockelmann K., Sigurdsson S., Abel T., 2007, *MNRAS*, 380, 1533
- Milosavljević M., Bromm V., Couch S. M., Oh S. P., 2009, *ApJ*, 698, 766
- Mirabel I. F., Dijkstra M., Laurent P., Loeb A., Pritchard J. R., 2011, *A&A*, 528, A149
- Mortlock D. J. et al., 2011, *Nature*, 474, 616
- Naoz S., Barkana R., 2007, *MNRAS*, 377, 667
- Navarro J. F., Frenk C. S., White S. D. M., 1996, *ApJ*, 462, 563
- Oh S. P., 2001, *ApJ*, 553, 499
- Oh S. P., Haiman Z., 2002, *ApJ*, 569, 558
- , 2003, *MNRAS*, 346, 456
- Ohkubo T., Nomoto K., Umeda H., Yoshida N., Tsuruta S., 2009, *ApJ*, 706, 1184
- Omukai K., Palla F., 2001, *ApJ*, 561, L55
- Omukai K., Schneider R., Haiman Z., 2008, *ApJ*, 686, 801
- Park K., Ricotti M., 2012, *ApJ*, 747, 9
- Peebles P. J. E., 1993, *Principles of Physical Cosmology*. Princeton University Press
- Petri A., Ferrara A., Salvaterra R., 2012, *MNRAS*, 422, 1690
- Regan J. A., Haehnelt M. G., 2009, *MNRAS*, 393, 858
- Ricotti M., 2009, *MNRAS*, 392, L45
- Ricotti M., Ostriker J. P., 2004, *MNRAS*, 352, 547
- Ricotti M., Ostriker J. P., Gnedin N. Y., 2005, *MNRAS*, 357, 207
- Salpeter E. E., 1955, *ApJ*, 121, 161
- Schleicher D. R. G., Spaans M., Glover S. C. O., 2010, *ApJ*, 712, L69
- Sesana A., Volonteri M., Haardt F., 2007, *MNRAS*, 377, 1711
- Sethi S., Haiman Z., Pandey K., 2010, *ApJ*, 721, 615
- Shakura N. I., Sunyaev R. A., 1973, *A&A*, 24, 337
- Shang C., Bryan G. L., Haiman Z., 2010, *MNRAS*, 402, 1249
- Shankar F., Croce M., Miralda-Escudé J., Fosalba P., Weinberg D. H., 2010, *ApJ*, 718, 231
- Shankar F., Salucci P., Granato G. L., De Zotti G., Danese L., 2004, *MNRAS*, 354, 1020
- Shankar F., Weinberg D. H., Miralda-Escudé J., 2009, *ApJ*, 690, 20
- Shapiro P. R., Iliev I. T., Raga A. C., 1999, *MNRAS*, 307, 203
- , 2004, *MNRAS*, 348, 753
- Shapiro S. L., 2005, *ApJ*, 620, 59
- Somerville R. S., Kolatt T. S., 1999, *MNRAS*, 305, 1
- Spaans M., Silk J., 2006, *ApJ*, 652, 902
- Stacy A., Greif T. H., Bromm V., 2010, *MNRAS*, 403, 45
- , 2012, *MNRAS*, 422, 290
- Tanaka T., Haiman Z., 2009, *ApJ*, 696, 1798
- Tanaka T., Menou K., 2010, *ApJ*, 714, 404
- Taniguchi Y., 2004, *Progress of Theoretical Physics Supplement*, 155, 202
- Tegmark M., Silk J., Rees M. J., Blanchard A., Abel T., Palla F., 1997, *ApJ*, 474, 1
- Tseliakhovich D., Barkana R., Hirata C. M., 2011, *MNRAS*, 418, 906
- Turk M. J., Abel T., O’Shea B., 2009, *Science*, 325, 601
- Turk M. J., Oishi J. S., Abel T., Bryan G. L., 2012, *ApJ*, 745, 154
- Turner E. L., 1991, *AJ*, 101, 5
- Ueda Y., Akiyama M., Ohta K., Miyaji T., 2003, *ApJ*, 598, 886
- Venkatesan A., Giroux M. L., Shull J. M., 2001, *ApJ*, 563, 1
- Volonteri M., Haardt F., Madau P., 2003, *ApJ*, 582, 559
- Volonteri M., Natarajan P., 2009, *MNRAS*, 400, 1911
- Volonteri M., Rees M. J., 2005, *ApJ*, 633, 624
- , 2006, *ApJ*, 650, 669
- Wechsler R. H., Bullock J. S., Primack J. R., Kravtsov A. V., Dekel A., 2002, *ApJ*, 568, 52
- Whalen D., Abel T., Norman M. L., 2004, *ApJ*, 610, 14
- Wheeler J. C., Johnson V., 2011, *ApJ*, 738, 163
- Willott C. J. et al., 2010a, *AJ*, 139, 906
- , 2010b, *AJ*, 140, 546
- Wise J. H., Abel T., 2008, *ApJ*, 685, 40
- Wolcott-Green J., Haiman Z., Bryan G. L., 2011, *MNRAS*, 418, 838
- Yoo J., Miralda-Escudé J., 2004, *ApJ*, 614, L25
- Yoshida N., Omukai K., Hernquist L., 2008, *Science*, 321, 669
- Zhang J., Fakhouri O., Ma C., 2008, *MNRAS*, 389, 1521
- Zhang W., Woosley S. E., Heger A., 2008, *ApJ*, 679, 639
- Zhao D. H., Jing Y. P., Mo H. J., Börner G., 2003, *ApJ*, 597, L9
- , 2009, *ApJ*, 707, 354